ELSEVIER

Journal of Structural Geology 26 (2004) 2191–2201

JOURNAL OF STRUCTURAL GEOLOGY

www.elsevier.com/locate/jsg

Progressive development of s-type flanking folds in simple shear

Ulrike Exner[a,*], Neil S. Mancktelow[a], Bernhard Grasemann[b]

[a]*Geologisches Institut, ETH-Zentrum, CH-8092 Zürich, Switzerland*
[b]*Institut für Geologische Wissenschaften, University of Vienna, A-1090 Vienna, Austria*

Received 11 November 2003; received in revised form 1 June 2004; accepted 1 June 2004

Available online 20 July 2004

Abstract

Flanking structures are deflections of planar or linear fabric elements in a rock alongside a crosscutting element (CE), e.g. a vein or fault. This study provides new results from analogue experiments, which test and extend recent numerical models of flanking structures. A linear viscous matrix material (PDMS) was deformed in a ring shear rig that allows continuous observation to large values of shear strain. Rotational behaviour, offset and deflection of marker lines around a predefined, lubricated CE were monitored for different initial orientations of the fault with respect to the shear zone boundary, and the results were compared with numerical results and natural examples. At high initial angles to the shear zone boundary ($>135°$), a structure previously described as an 's-type flanking fold' develops. During progressive deformation, an initially straight marker line passing through the centre of the CE is offset in a sense synthetic with the bulk sense of shear and shows a shortening displacement across the CE. Simultaneously, this central marker line is deflected and forms symmetrical folds, which are convex in the direction of shear along the CE (i.e. normal drag). Both offset and deflection of the marker lines decrease towards the tips of the fault. Natural examples of s-type flanking folds, directly comparable with the model results, are more common than is generally appreciated.
© 2004 Elsevier Ltd. All rights reserved.

Keywords: Analogue modelling; Fault-related folds; Flanking structures; Simple shear

1. Introduction

Several descriptive and numerical modelling studies concerning the deflection of planar passive markers around a discontinuity in a rock volume have been presented within the last few years (e.g. Grasemann and Stüwe, 2001; Passchier, 2001; Grasemann et al., 2003). These studies have introduced the general term *flanking structures*, reflecting the geometrical characteristic that they all show a symmetrical bending of marker lines around a planar central element, which is a structural or rheological discontinuity.

In describing the geometry of the different structures, we follow the terminology used in previous publications (Fig. 1). The planar discontinuity in the centre of a flanking structure is called the *crosscutting element* (CE; Passchier, 2001). It is embedded in a homogeneous matrix, which is highlighted by passive marker lines (in 2D view) aligned parallel to the shear zone boundary (SZB). The marker line crossing the CE at its centre in the undeformed state is defined as the *central marker line* (CML). Generally, three types of flanking structures exist, namely a-type flanking folds, s-type flanking folds and shear bands. For a-type flanking folds there is an antithetic displacement of the central marker line along the CE, whereas s-type flanking folds and shear bands are defined by a displacement synthetic to the bulk shear sense. The offset of the CML is contractional for s-type flanking folds and extensional for shear bands, whereas a-type flanking folds can show either contractional or extensional offset. The numerical study of Grasemann et al. (2003) showed that each of these three major groups could be further subdivided into two varieties, namely normal and reverse drag structures. The term *drag* is used in the sense of Hamblin (1965), according to which the drag of markers along the CE can be either *normal* or *reverse*, corresponding to a deflection convex or concave in the direction of shear along the CE. The development of flanking structures is dependent on (1) the initial orientation of the discontinuity and (2) the bulk flow geometry (see figs. 5 and 6 of Grasemann et al. (2003) for details).

Previous analogue studies (Hudleston, 1989; Odonne,

* Corresponding author. Tel.: +41-1-6323702; fax: +41-1-6321080.
E-mail address: ulrike.exner@erdw.ethz.ch (U. Exner).

0191-8141/$ - see front matter © 2004 Elsevier Ltd. All rights reserved.
doi:10.1016/j.jsg.2004.06.002

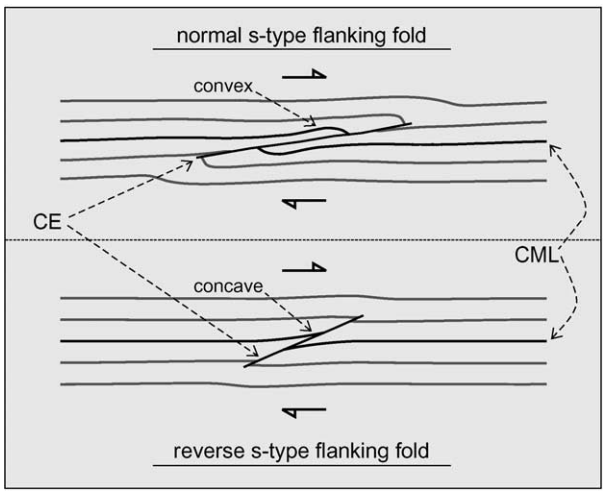

Fig. 1. Two different kinds of s-type flanking folds (normal and reverse). The crosscutting element (CE) is dipping against the shear direction. The sense of shear along the CE is in both cases synthetic to the bulk shear sense. Note the difference in drag of the central marker lines (CML).

1990; Koyi and Skelton, 2001) analysed the development of folds around pre-defined fault surfaces. All of these models show reverse a-type flanking folds or reverse shear bands, which are perfect mirror images in pure shear deformation (fig. 3 of Grasemann et al., 2003). The present study focuses on the formation of s-type flanking folds (Fig. 1), which are those showing an offset of the central marker line that is synthetic to the bulk kinematics of the shear zone. Since the drag along the CE can be either normal or reverse, there are two types of s-type flanking folds. In contrast to shear bands, which show an extensional offset of the central marker line, s-type flanking folds always have a contractional offset. However, it is important to note that in this case the terms *extensional* and *contractional* are only related to the offset of the marker lines and do not necessarily apply to the flow geometry of the whole shear zone. For example, s-type flanking folds can form in overall simple shear, in which there is no bulk stretch or shortening parallel to the shear zone boundary.

The development of such s-type flanking structures is important because, if correctly recognised and interpreted, they can be used as kinematic indicators in well-constrained natural examples. Natural s-type flanking structures are found in a wide range of tectonic environments and rock types. This new type of fault-related fold is actually quite common, but the characteristic geometry has been often overlooked, because its mechanical significance was not recognised.

2. Analogue materials and methods

The analogue experiments were conducted in the ring shear apparatus described by Arbaret et al. (2001). This machine consists of two concentric vertical cylinders of different diameter, which rotate with the same angular velocity but in opposite directions. The resulting flow geometry can be described as cylindrical Couette flow, which approximates plane strain simple shear with decreasing shear strain rate $\dot{\gamma}$ from the inner to the outer cylinder. The shear strain rate for a point at the radius r can be calculated as follows (e.g. Reiner, 1969):

$$\dot{\gamma} = \frac{-2\left(\dot{\Omega}_i - \dot{\Omega}_e\right)}{r^2\left(\frac{1}{r_i^2} - \frac{1}{r_e^2}\right)} \quad (1)$$

where r_i is the radius of the inner cylinder (176 mm), r_e the radius of the outer cylinder (300 mm), and $\dot{\Omega}_i$ and $\dot{\Omega}_e$ are the corresponding angular velocities.

The analogue material between the two cylinders rests on a higher density lubricant layer (glycerine) at the bottom of the apparatus. A transparent polymer PDMS (polydimethyl siloxane SGM 36, manufactured by Dow Corning) was used as the matrix material. For the experimental conditions of this study (~22 °C, shear strain rate $7.7 \times 10^{-4}\ s^{-1}$ in the centre of the shear zone), PDMS is effectively Newtonian linear viscous, with a viscosity of $3–5 \times 10^4$ Pa s (see Weijermars (1986) and ten Grotenhuis et al. (2002) for details). As a consequence, brittle initiation and propagation of a fault (as CE) cannot be modelled with this analogue material. Therefore, a 2-mm-wide, 2-cm-long and ca. 2-cm-deep vertical cut was made in the PDMS. Lubrication of the cut was achieved with two different materials: (1) liquid soap with a density slightly less than PDMS, and an effective viscosity approximately 5×10^4 less than the matrix material; and (2) transparent silicone oil with a density in the range of PDMS, but a significantly lower effective viscosity. Initial experiments used liquid soap, following the approach of Marques and Coelho (2001), Mancktelow et al. (2002) and Ceriani et al. (2003). However, liquid soap alone is not capable of maintaining the cut as a continuous slip surface. To maintain slip, it was necessary to place an additional piece of overhead transparency in the cut, the same size as the cut itself. The liquid soap then acted as a lubricant along the 'fault' surface provided by the foil. Tests during the course of the study established that silicone oil alone could maintain a continuous slip surface and this lubricant was subsequently employed. However, both experimental setups ensure that the 'fault' remains an active slip surface during the experiment, and the results from repeated runs are identical.

The deformation of the matrix material around the CE was tracked using a marker grid imprinted on the surface of the model using partially fixed photocopies (Dixon and Summers, 1985). The setup using soap rather than silicone oil was preferred for photographic documentation and further processing, as it was easier to obtain a marker grid imprint in the immediate vicinity of the cut. During the course of an experiment, high-resolution pictures were taken with a digital camera every 3 min.

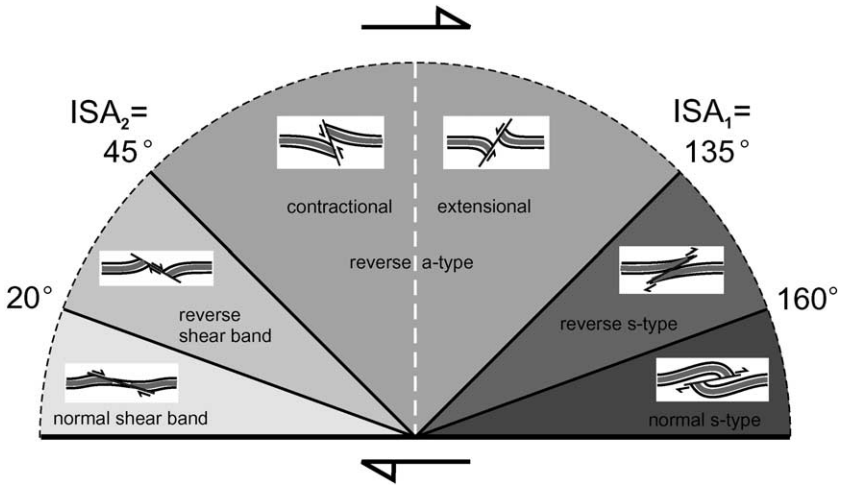

Fig. 2. The development of different flanking structures under simple shear conditions, depending on the initial angle ϕ of the CE to the shear zone boundary (after Grasemann et al., 2003). Note that this diagram is valid exclusively for a dextral sense of shear (the case for sinistral shear is mirror-symmetric across the vertical plane). The diagram also only indicates the type of structure that would develop *instantaneously* from initially planar marker layers continuous across the CE. Note that the shear sense along the CE is reversed as its orientation passes through that of the instantaneous stretching axes at 45° (ISA_2) and 135° (ISA_1), respectively.

3. Results from analogue modelling

3.1. S-type flanking folds

Under simple shear boundary conditions, the instantaneous structure development is determined by the initial angle ϕ of the discontinuity to the shear zone boundary. Based on the numerical modelling study by Grasemann et al. (2003), Fig. 2 summarises the various structures that should develop in different sectors for dextral simple shear (i.e. the same as the experiments).

If the CE is oriented at low angles to the SZB,[1] shear bands are formed. Between 45 and 135° to the SZB, deflection of the marker lines results in a-type flanking fold geometries, with contractional offset below 90° and extensional offset above 90°. Initial angles higher than 135° to the SZB generate s-type flanking folds, which can again be subdivided into reverse and normal drag structures. The latter occur at ϕ-angles above 160°. As the discontinuity itself co-rotates in simple shear, one structure can in principle evolve from the previous one and if the shear strain is sufficient, all flanking structures should end up in the field of normal s-type flanking folds. However, it is unlikely that a discontinuity initially inclined at a low angle to the SZB (e.g. 15°, initially forming a normal drag shear band) would finally display perfect normal s-type geometry, since the distortion of marker lines would be too complex after more than 140° of rotation.

S-type flanking folds, as considered in the current study, develop around discontinuities that are initially oriented at a high angle to the SZB. Between 135 and 160°, the resulting structure is defined as a 'reverse drag s-type flanking fold'. Reverse drag refers to the curvature of the CML, which is *reverse* (in this case concave) when compared with the *normal* case (convex curvature) expected for the sense of shear along the CE (Reches and Eidelman, 1995). The change between reverse and normal drag occurs at an angle around 160°. Both reverse and normal s-type flanking folds are characterised by a contractional offset of the CML. This feature clearly distinguishes these structures from shear bands, which always show extensional offset of the CML.

We prefer the term contractional fault instead of thrust or reverse fault, because all deformation around the CE is compensated locally and, at a certain distance from the centre, the effect of the discontinuity is zero. For simple shear, there is therefore no overall shortening or stretching of material lines parallel to the SZB. In addition, 'normal' and 'reverse' is associated with down dip movement and this terminology would be inappropriate for flanking folds related to vertical faults with strike-slip displacement.

In Fig. 3, analogue experiments of s-type flanking folds at initial angles of $\phi = 140$ and 160° are compared with equivalent numerical models (Grasemann et al., 2003) conducted with the finite element code BASIL (Barr and Houseman, 1996). At an initial angle of $\phi = 140°$ of the CE to the SZB, the development of a reverse s-type flanking fold can be observed (Fig. 3a). The CML is deflected with a concave curvature, while simultaneously the CE shows a dextral offset, synthetic with the sense of the bulk shear zone. During progressive dextral shear, the offset of the CML along the CE increases, but the concave deflection transforms into a convex one. The exact stage at which this change from reverse to normal drag occurs is not easy to determine, since it is a subtle transition from a weak

[1] The convention followed in this study is that positive angles are measured in the same direction as the bulk rotation.

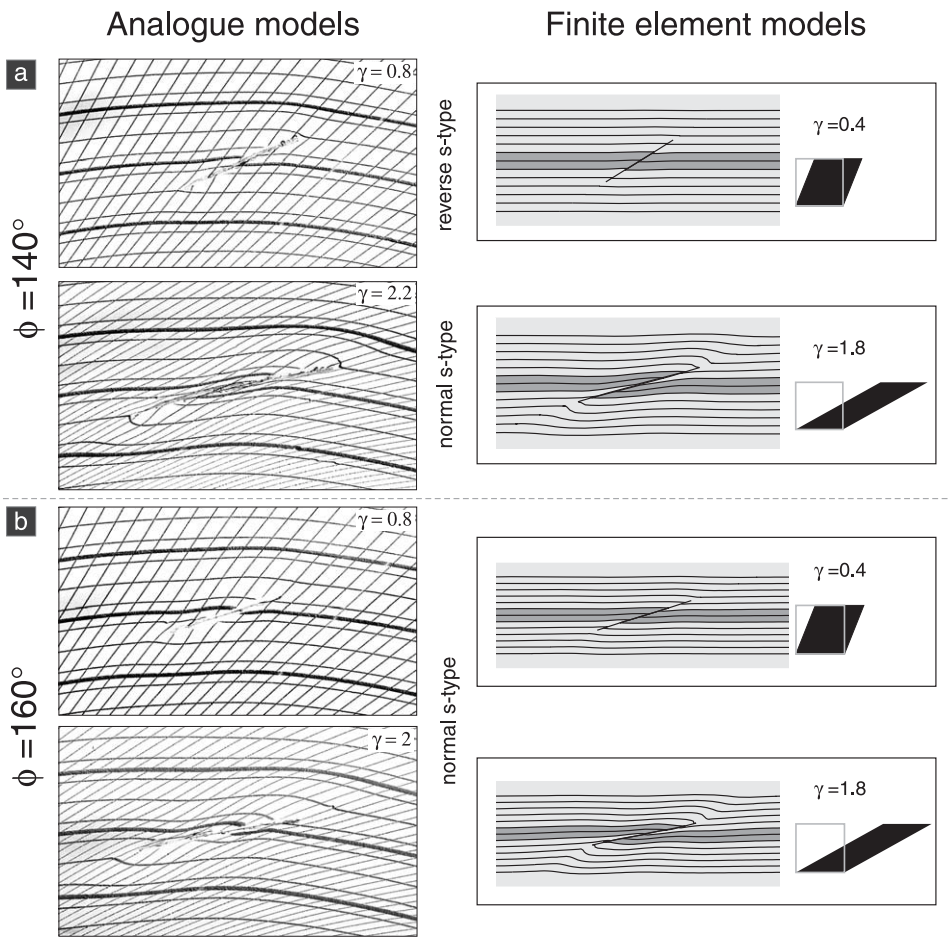

Fig. 3. (a) Numerical vs. analogue experiments for a CE with an initial angle $\phi = 140°$ to the shear zone boundary. A reverse s-type flanking fold quickly evolves into a normal s-type flanking fold at $\gamma \sim 1$. (b) Numerical vs. analogue experiments for a CE with an initial angle $\phi = 160°$ to the shear zone boundary. A normal s-type flanking fold is visible from the very beginning of the experiment.

synform to an (initially) also weak antiform. However, at a shear strain of $\gamma \sim 1.3$, the normal drag is clearly visible, and becomes progressively more pronounced. In contrast, in the other experiment with an initial angle of $\phi = 160°$, a normal drag can be observed from the onset of deformation (Fig. 3b), which is consistent with the results from numerical modelling summarised in Fig. 2.

A closer look at the progressive development of s-type flanking folds for various initial angles reveals that the drag of marker lines is not necessarily consistent over the length of the CE. The central marker line of the normal drag s-type flanking fold at $\gamma = 2.2$ (Fig. 3a) shows normal drag and two-fold rotational (or point) symmetry around the midpoint of the CE. Moving towards the tips, the flanking fold is still point symmetric on the scale of the whole structure, but adjacent features across the CE are markedly different, displaying (weak) normal drag on one side and clear reverse drag on the other. This highlights the importance of the CML in any interpretation of natural flanking structures, observations from tip regions alone can lead to false interpretations.

The rotation of the CE can be compared with the rotation of a rigid monoclinic particle in a viscous matrix. Analytical, numerical and analogue studies have shown that the rotation rate of such an inclusion is high at angles near 90° to the SZB and low at acute angles (e.g. Jeffery, 1922; Ghosh and Ramberg, 1976; Arbaret et al., 2001). Moreover, in simple shear, lubrication of the inclusion interface leads to a stabilisation at a small angle inclined against the sense of shear (Mancktelow et al., 2002; Ceriani et al., 2003). This behaviour can also be observed in our experiments, where the lubricated inclusion is replaced by a lubricated fault, which asymptotically approaches a similar small angle to the SZB (Figs. 4 and 7b).

One of the findings of these analogue experiments is that s-type flanking folds are small-strain structures, generally recognizable only at $\gamma < 3$. Above this value, a rigorous interpretation becomes impossible (Fig. 5) for the following reasons:

1. The CE is no longer distinctly visible. It becomes extremely thin as a result of progressive stretching during deformation.
2. The grid lines in the experiments (as well as similar marker lines in natural examples) become increasingly distorted, and single lines are no longer clearly visible.

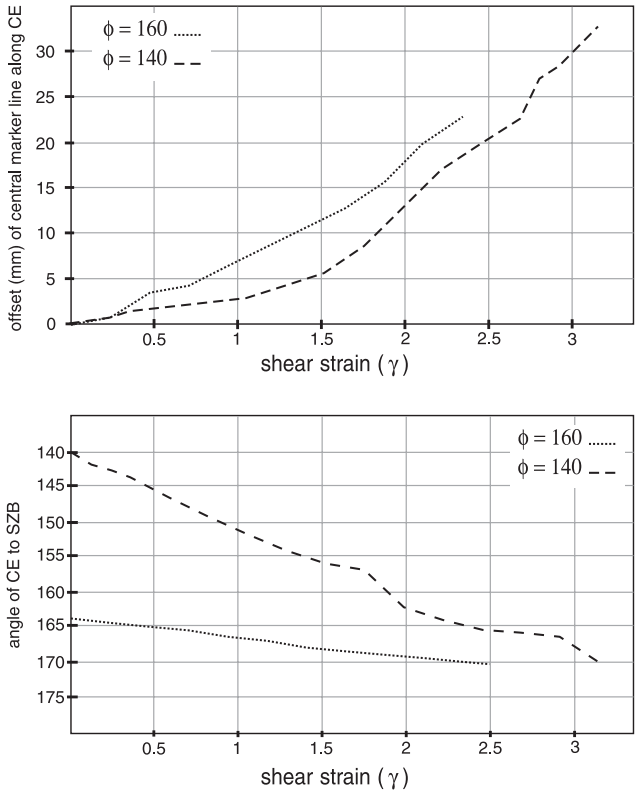

Fig. 4. Plots of shear strain against offset of the CML along the CE and the angle of the CE to the shear zone boundary, respectively. Both experiments in which s-type flanking folds developed (with initial angles of the CE to the SZB of 140 and 160°, respectively) are shown.

3. The limbs of the folds outlined by passive marker lines become sub-parallel and increasingly appressed as they rotate into the shear zone and are stretched together with the CE.
4. The curvature of the CE increases, which can be attributed to the boundary conditions of the ring shear apparatus. All marker lines initially parallel to the radii of the two cylinders are not only stretched, but also become curved during deformation (see fig. 2 of Arbaret et al., 2001).

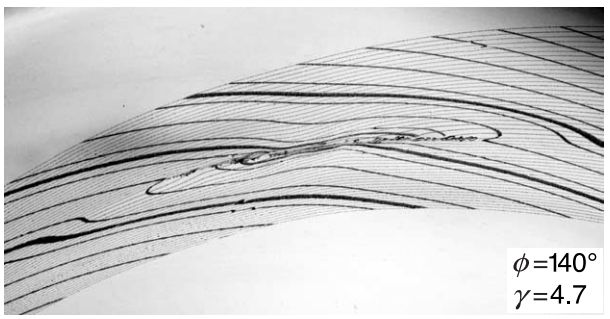

Fig. 5. Structure developed from a normal s-type flanking fold ($\phi = 140°$) at $\gamma \sim 4.7$. Note that the CML is subparallel to the CE, and may be indiscernible in natural field examples.

3.2. Progressive development of s-type from reverse a-type flanking folds

In simple shear, a CE initially sub-perpendicular to the shear zone boundary ($\phi \sim 90°$; Fig. 6a) results in the development of a reverse a-type flanking fold (Grasemann et al., 2003), which is characterised by antithetic displacement of passive marker lines along the CE (Fig. 6b and c). During progressive shear, the CE rotates through the principal instantaneous stretching axis (ISA_1) at 135° (Passchier and Trouw, 1996) and the sense of shear along the fault switches to synthetic. From this orientation onwards, the offset of the central marker line decreases, while the flexure close to the CE remains more or less constant in shape (Fig. 6d and e). Eventually a temporary geometry occurs with no offset of the central marker line (Fig. 6f), which strongly resembles n-type flanking folds (characterised by no displacement along the CE; Passchier, 2001). Subsequently, an s-type flanking fold with increasing synthetic displacement of the central marker line develops (Fig. 6g and h).

Fig. 7a summarises, for progressively increasing shear strain, the relationship between the offset of the CML along the CE and the angle of the CE to the SZB, in an experiment with an initial angle $\phi = 90°$. The initial offset of the CML is sinistral and therefore antithetic to the bulk dextral shear sense. At $\gamma \sim 1–1.4$, the maximum antithetic offset is achieved. After a period of stagnation, the sense of shear along the CE is reversed, and becomes synthetic to the bulk shear sense. The subsequent stage is characterised by decreasing throw, finally reaching zero at $\gamma \sim 2.3$. Synthetic shearing results in the formation of a normal s-type flanking fold. The temporary reverse s-type geometry postulated in Fig. 2 (or fig. 5 of Grasemann et al., 2003) is not developed. This can be ascribed to the pre-existing convex curvature of the CML, which does not allow a transient and subtle concave deflection to develop. The rate of synthetic offset is initially of similar magnitude to the previous antithetic one, but decreases for $\gamma > 3.5$. In a plot of the angle of the CE to the SZB against γ (Fig. 7b), this decrease in displacement rate along the CE correlates with a reduction in the rotation rate of the CE, which approaches the SZB asymptotically. Similar to s-type flanking folds developing at an initial angle $\phi > 135°$, s-type flanking folds evolved from a-type flanking folds become increasingly deformed. For $\gamma > 4$, the structure becomes unrecognisable (Fig. 5), and an interpretation is impossible, particularly if the previous deformation history is not known.

Development of unambiguous s-type flanking folds is dependent on the initial angle of the CE to the SZB. If this angle is less than ~50°, the deflection and especially the throw of the marker lines in the preceding a-type stage are too great, so that after passing the stretching ISA_1, lengthening of the whole structure rather than slip along the CE is observed (Fig. 8a; see also the comparable natural

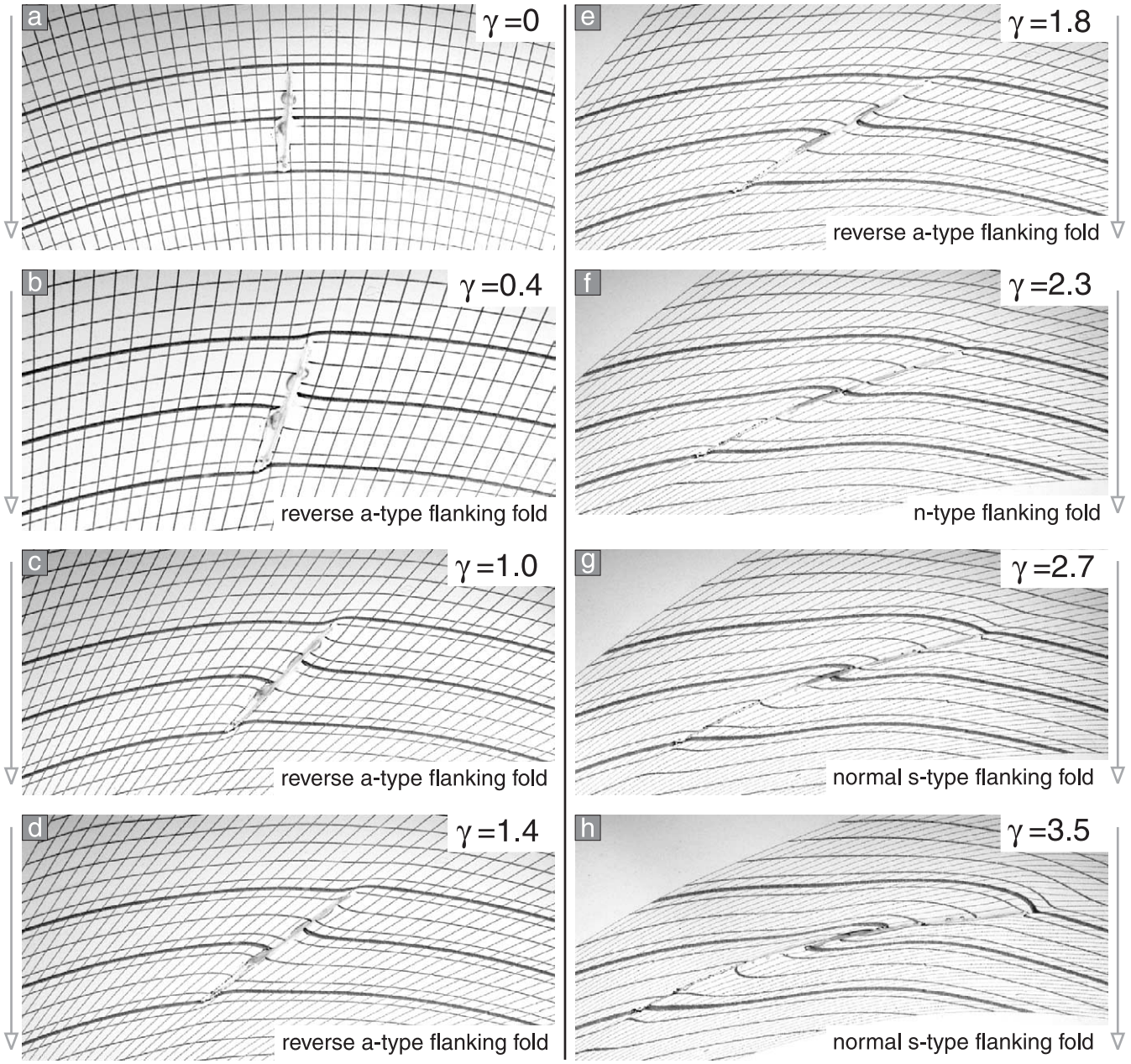

Fig. 6. Analogue experiment with initial angle $\phi = 90°$, demonstrating the progressive development from a reverse a-type flanking fold to a normal drag s-type flanking fold in dextral simple shear. For details of the progressive development of γ and ϕ see Fig. 7.

example of Fig. 8b). Another important factor for the evolution of s-type flanking folds from precursory a-type flanking folds is the lubrication of the CE. If the lubricating substance has been consumed in an early stage, only rotation of the CE is observed, and the slip necessary for transition to s-type geometry no longer occurs. This may also be relevant in nature if the fracture eventually heals.

3.3. Comparison with FEM-results

Comparing the analogue models of this study, conducted in a ring shear apparatus, with the numerical models for simple shear flow (Fig. 3; Grasemann et al., 2003), there is in general a good correspondence between the results, although some differences can be noted. For the same initial conditions, both numerical and analogue models produce identical flanking structure geometries, although the radial gradient in shear strain rate in the ring shear apparatus does result in additional curvature and asymmetry that become increasingly pronounced with higher γ. For example, when $\gamma = 5$ at the centre of the shear zone, $\gamma = 4.61$ or 5.45 at positions 1 cm closer to the outer and inner shear zone boundaries, respectively. However, a major advantage of the analogue experiments is that there is no limit to the amount of strain that can be achieved. In particular, the progressive development from initial a-type to subsequent

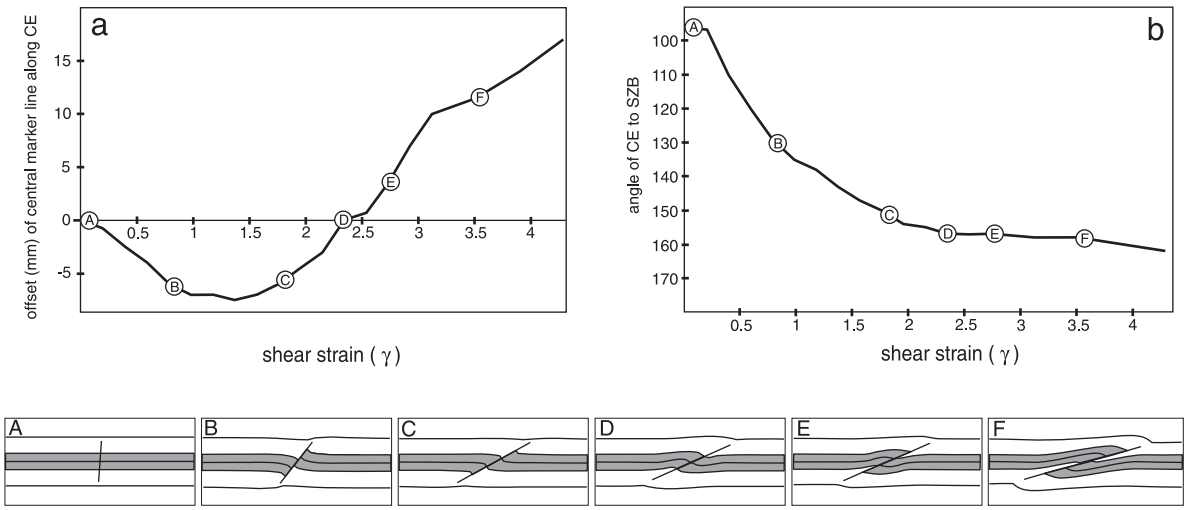

Fig. 7. (a) Plot of offset of CML along CE (in mm) vs. γ for initial angle $\phi = 90°$. (b). Plot of offset of CML along CE (in mm) vs. angle of CE to shear zone boundary (SZB) for $\phi = 90°$. Compare with modelled structures in Fig. 6.

s-type flanking folds with increasing shear strain could not be observed in the published finite element models, because of the limitation in achievable shear strain (Grasemann et al., 2003). However, higher strain in finite element models could also be attained if a remeshing algorithm was introduced.

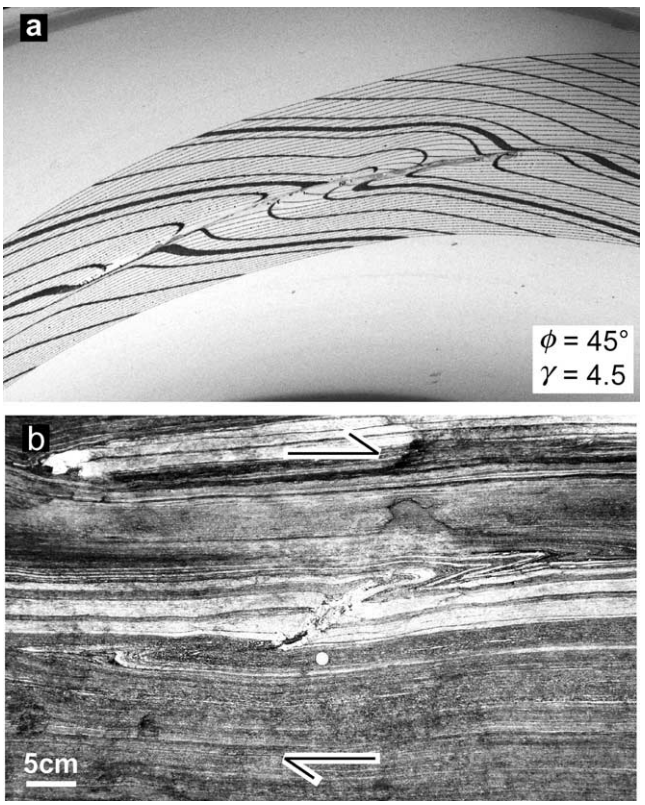

Fig. 8. (a) Analogue experiment with initial angle $\phi = 45°$ at $\gamma \sim 4.5$. The structure would be interpreted as an a-type flanking fold, even though it is presently in the sector of instantaneous s-type development. (b) Possible natural example of such a large-strain a-type flanking fold (photograph taken at the same outcrop as Fig. 9).

4. Natural examples

In order to apply and test the insights gained from the models presented above, natural examples of s-type flanking folds have been sought for direct comparison. These are actually more common than is generally recognised. Occurrences of normal s-type flanking folds have been documented for scales spanning several orders of magnitude and for rocks from all metamorphic grades, even including slump structures in non-metamorphic sediments (fig. 9b of Grasemann et al., 2003).

Fig. 9a shows a small-scale example of a reverse s-type flanking fold from the border of the Monte Rosa nappe in the Italian Alps. The dextral sense of shear in this outcrop is independently established by other shear sense criteria, e.g. σ-type porphyroclasts (cf. Simpson and Schmid, 1983). The central discontinuity terminates at both ends without bending into a foliation-parallel detachment zone.

The field of reverse s-type flanking folds is not very broad in simple shear ($\phi = 135–160°$) and becomes even narrower in general shear transpression (Grasemann et al., 2003). Therefore, natural marker lines around such CEs would initially have to be exceptionally planar and parallel, otherwise the subtle deflection would not be noticeable. In addition, the experiment presented in Fig. 6 clearly establishes that if there is a reverse a-type precursor structure, a subsequent stage of reverse s-type flanking fold development is not observed.

Nevertheless, reverse s-type flanking folds might be more common in transtensional general shear geometries, where this type of structure already forms at smaller angles of the CE to the SZB (pers. comm. G. Wiesmayr). Fig. 9b shows a clear reverse s-type flanking fold from the same outcrop as Fig. 9a. This structure is more likely to develop in transtensional general flow, as the current angle of the CE to the SZB is smaller than 135°.

A large-scale example from amphibolite facies rocks of

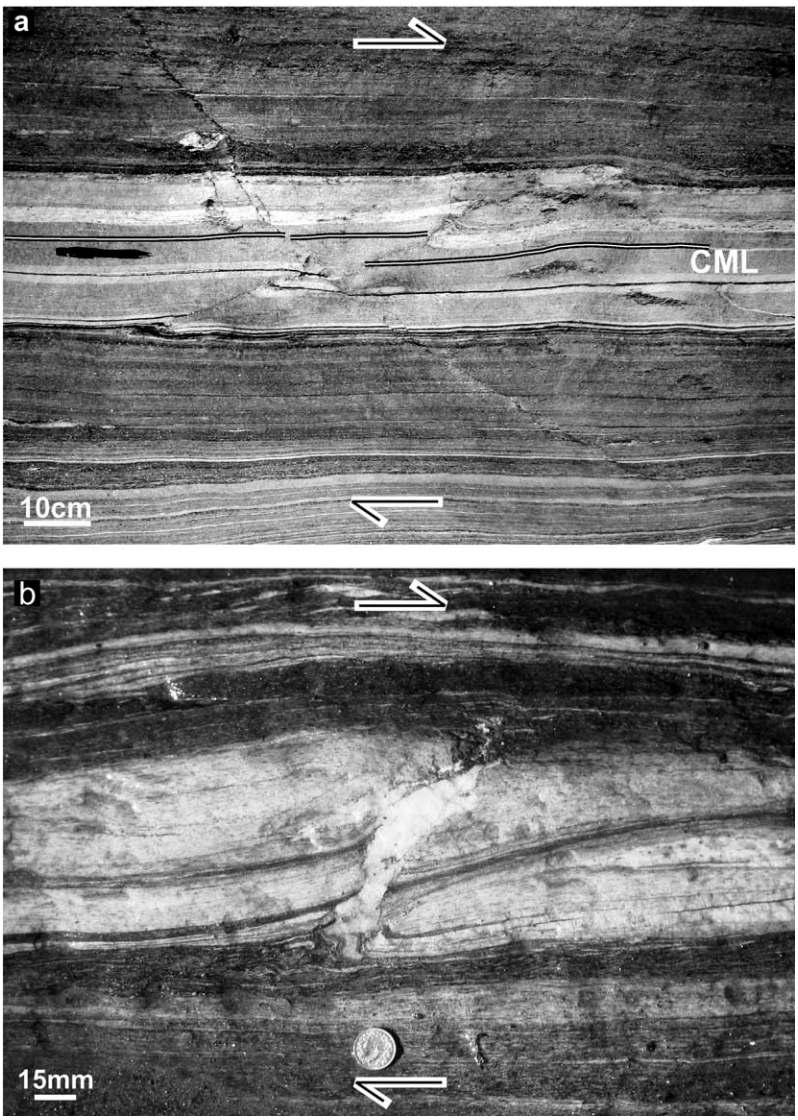

Fig. 9. Natural examples of reverse s-type flanking folds in highly deformed paragneisses from the border of the Monte Rosa nappe, Villadossola (Italian Alps). (N 46° 04′ 07.7″, E 08° 15′ 14.3″). The dextral sense of shear is known from independent shear sense indicators.

the Schneeberg Complex in northern Italy shows the deflection of a quartzitic layer to either side of a fault surface (Fig. 10a). The full length of the CE actually extends beyond the borders of the photograph, but based on constraints from structural mapping, the quartzitic layer roughly represents the true central marker of the structure. The structure is thus interpreted as a normal s-type flanking fold. The offset along the CE is synthetic with the regional (sinistral) sense of shear (pers. comm. H. Soelva).

Fig. 10b shows a block from a marble quarry in the Ivrea Zone, Italian Alps (photograph courtesy of L. Burlini). It contains an amphibolite layer, which forms two well-developed normal s-type flanking folds. Numerous other more-or-less vertical fractures of the competent layer suggest that initially the CEs of these two s-type flanking folds formed as faults with an orientation nearly perpendicular to the layering.

As is true of all flanking structures, reverse s-type flanking folds can easily be confused with their mirror images, i.e. contractional a-type flanking folds. Contractional a-type flanking folds develop at medium angles (for simple shear, at initial angles between 45 and 90°) of the CE to the SZB, but have a sense of shear along the CE antithetic to the bulk shear sense. Thus, it is necessary to independently establish the sense of shear by other kinematic criteria or from several different flanking structures (with various initial angles of the CE) if a correct interpretation of the natural structure is to be made.

Natural examples of s-type flanking folds developed from preceding reverse a-type flanking folds are hard to document unequivocally, because finite structures do not retain much evidence of their previous history. Nevertheless, the geometry of some a-type flanking folds (e.g. Fig. 10c) strongly suggests that their continued evolution during ongoing deformation would be similar to the one observed in the analogue models (Fig. 6). The most common

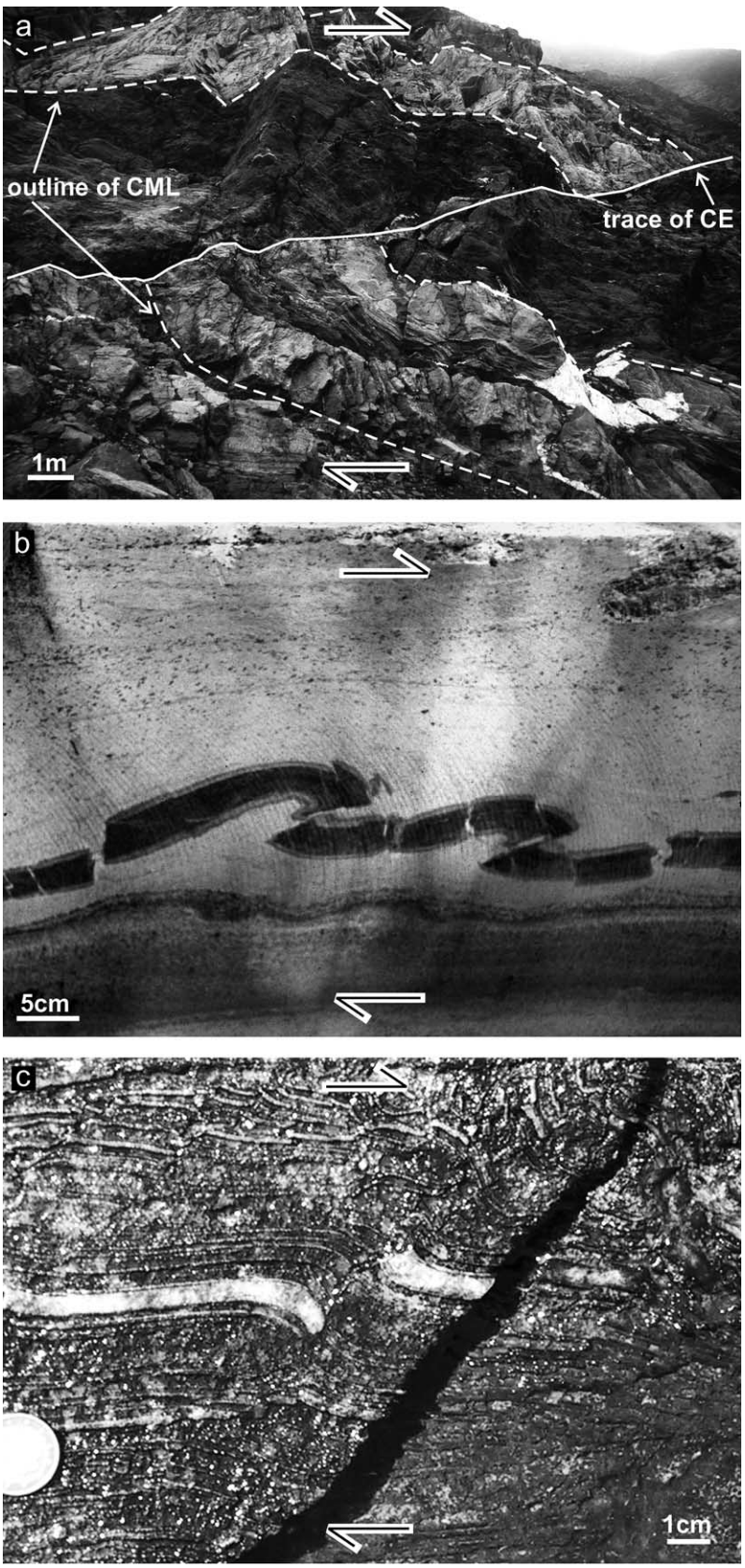

Fig. 10. (a) Large-scale normal s-type flanking fold in a quartzitic layer under amphibolite facies metamorphic conditions, Schneeberg Complex, Italian Alps (N 46° 45′ 25.2″, E 11° 01′ 42.5″). The field photograph has been reversed to allow direct comparison with the dextral sense of all other structures shown in this study. (b) Normal s-type flanking folds of amphibolite layer in marble (Ivrea Zone, Italy; N 45° 45′ 00″, E 08° 25′ 40″). Photograph courtesy of Luigi Burlini. (c) Reverse a-type flanking fold in layered calcite-dolomite marble, Naxos, Greece (N 36° 58′ 15.1″, E 025° 24′ 22.3″).

orientation for initial fracture development observed in natural examples is at a high angle to the foliation and lineation, where the fractures represent extensional joints. This suggests that many natural normal s-type flanking folds may have had a development similar to Fig. 6, i.e. with an a-type precursor.

5. Discussion

The analogue experiments presented in this study illustrate the evolution of s-type flanking structures under cylindrical Couette flow, which is a close approximation to simple shear (but with a radial decrease in shear strain rate). Such s-type flanking structures developed around a central discontinuity are also observed in natural shear zones. The results from analogue models confirm previous numerical studies, but provide additional information on the evolving geometries for shear strains larger than $\gamma \sim 2–3$.

Passchier (2001) describes several mechanisms for the formation of flanking structures. His fig. 8.IV, which shows an s-type flanking fold at the margin of a dyke or vein, was explained by ductile shearing within or at the borders of the intrusion. The resulting strain gradient to the external host rock produces the deflection of the layering in a flanking fold-geometry. Our analogue models reveal the progressive development of this strain gradient in detail and correspondingly explain the development of the modelled flanking folds by perturbation strain (Baumann and Mancktelow, 1987; Mancktelow, 1991), which is generated by slip along the CE. The different vorticity number (W_k) within the CE and its rotation result in a local disturbance in the far-field homogeneous flow. This deviation must be compensated in the matrix adjacent to the central discontinuity, producing a deflection of the marker lines.

For the correct interpretation of flanking structures, some preconditions have to be fulfilled. The unambiguous identification of a *central marker line* is of great importance, as deflection and offset of marker lines vary along the length of the CE. A close look at the geometry of normal s-type flanking structures reveals that (1) the offset of the marker lines decreases towards the tips of the CE, whereas at the same time (2) the folding of the marker lines becomes more open (the wavelength increases). Moreover, the drag of the marker lines may change along the CE (Reches and Eidelman, 1995). At $\gamma = 2.2$ in the analogue model and $\gamma = 1.8$ in the FEM, respectively (Fig. 3a), the drag of the central marker line is normal, whereas the marker line below it (on the left side) shows a reverse drag. This demonstrates that it is essential to identify the tips of the CE and thereby define the position of a true central marker line, i.e. a (possibly imaginary) line at the symmetry centre of the flanking structure. In some cases, the most conspicuous deflected marker lines may draw attention to a section of the structure that is not suitable for unequivocal interpretation. In other cases, if the single layers are very similar in thickness and colour, it might be difficult to match the correct marker lines on either side of the CE. Some examples of flanking structures may also be difficult to interpret because the length of the CE is not clear. To decide where the tips of the CE might be, it is necessary to find marker lines that show deflection but no offset. Another helpful criterion to decide whether a structure is fully exposed is to analyse the overall symmetry, since a two-fold (or point) symmetry axis is a precondition for interpreting fault-related folds as flanking structures. An arbitrary and possibly incomplete section will show misleading drag effects on both sides of the CE and a correct evaluation of incomplete flanking structures is therefore difficult or even impossible.

Essential for the formation of s-type flanking folds (and also a-type flanking folds and shear bands) is the necessity for slip on the CE, otherwise an n-type flanking fold (i.e. no slip) will develop. In analogue experiments, slip conditions along the CE were provided by a thin film of liquid soap or silicone oil. In natural rocks, such lubricating effects might be accomplished by a fluid present on the CE or by a weaker material, which facilitates the localisation of deformation along the CE. The weaker material behaviour along the CE could be due to a finer grain size, possibly due to dynamic recrystallisation (e.g. Poirier, 1980) or compositional differences (e.g. calcite veins in sandstone or chlorite veins in granite). The influence of viscosity contrast between CE and matrix on the geometry of flanking folds has already been discussed in some detail by Grasemann and Stüwe (2001).

The progressive development from reverse a-type to normal s-type flanking structures (Fig. 6) shows a switch from an extensional to a contractional structure in a single model run, without any variation of the boundary conditions of the shear zone. Thus, care must be taken concerning the interpretation of ‘finite’ structures observed in natural rocks, since these do not directly reflect the ‘instantaneous’ stages summarised in Fig. 2. In Fig. 6, for example, a-type geometries are preserved well into the instantaneous s-type field and n-type geometry is also developed during subsequent transition to eventual true s-type geometries. In order to avoid misinterpretations, if possible more than one structure with differently oriented CEs within the shear zone should be investigated, based on the reasonable assumption that variations in finite strain might reveal the progressive structural evolution.

An s-type flanking fold is a low-strain structure. It is metastable and evolves with increasing γ into a complex structure, which resembles an intrafolial fold (i.e. not clearly related to a fault or discontinuity) rather than an obvious flanking fold. Most of the investigated natural examples of s-type flanking folds developed in layered rocks of apparently rather low rheological contrast between the layers. The layers provide markers outlining the flanking fold geometry, but were not mechanically important in their development.

6. Conclusions

The development of s-type flanking folds has been documented in both analogue and numerical models. During progressive deformation, an initially straight line parallel to the SZB across the centre of a planar discontinuity (the 'central marker line') shows a contractional displacement, synthetic with respect to the sense of the shear zone. Simultaneously, this central marker line is deflected and forms symmetrical folds, which are convex in the direction of shear along the CE. The offset of the marker lines decreases towards the tips of the fault. S-type flanking folds record a *local* contractional displacement of the marker lines parallel to the SZB, although the imposed deformation is effectively simple shear. If not recognised as such, s-type flanking folds can be misinterpreted as fault-related folds associated with a significant shortening component parallel to the SZB. The results from analogue experiments confirm the earlier numerical studies, but extend the results to higher shear strains ($\gamma > 3$). Progressive development from reverse a-type to normal s-type flanking folds involves a switch from extensional to contractional offset. The transitional geometry between these two clearly discernable structures can easily be confused with 'n-type' flanking folds (where there is no slip along the CE). Thus, care must be taken concerning the interpretation of 'finite' structures in natural rocks, as they may be transient. Further deformation under constant boundary conditions could lead to a quite different geometry.

Acknowledgements

The Flash Team, especially C. Passchier, G. Wiesmayr and T. Kocher, is thanked for many lively discussions both in the field and in the lab. Thanks to S. Ceriani for passing on his practical experience with the ring shear apparatus. R. Hofmann is acknowledged for initially constructing and now maintaining the ring shear apparatus and U. Gerber for frequent assistance with the digital photographs. Discussion with A. Barnhoorn is greatly appreciated. L. Burlini provided the photograph of Fig. 10b. This work was supported by the ETH project 0-20998-02 and Austrian Science Foundation FWF project P-15668-Geo. We would also like to acknowledge constructive and thorough reviews by P. Cobbold and D. Grujic.

References

Arbaret, L., Mancktelow, N.S., Burg, J.-P., 2001. Effect of shape and orientation on rigid particle rotation and matrix deformation in simple shear flow. Journal of Structural Geology 23, 113–125.

Barr, T.D., Houseman, G.A., 1996. Deformation fields around a fault embedded in a non-linear ductile medium. Geophysical Journal International 125, 473–490.

Baumann, M., Mancktelow, N.S., 1987. Initiation and propagation of ductile shear zones. Terra Cognita 7(1), 47.

Ceriani, S., Mancktelow, N.S., Pennacchioni, G., 2003. Analogue modelling of the influence of shape and particle/matrix interface lubrication on the rotational behaviour of rigid particles in simple shear. Journal of Structural Geology 25, 2005–2021.

Dixon, J.M., Summers, J.M., 1985. Recent developments in centrifuge modeling of tectonic processes: equipment, model construction techniques and rheology of model materials. Journal of Structural Geology 7, 83–102.

Ghosh, S.K., Ramberg, H., 1976. Reorientation of inclusions by combination of pure shear and simple shear. Tectonophysics 34, 1–70.

Grasemann, B., Stüwe, K., 2001. The development of flanking folds during simple shear and their use as kinematic indicators. Journal of Structural Geology 23, 715–724.

Grasemann, B., Stüwe, K., Vannay, J.-C., 2003. Sense and non-sense of shear in flanking structures. Journal of Structural Geology 25, 19–34.

Hamblin, W.K., 1965. Origin of "reverse drag" on the downthrown side of normal faults. Geological Society of America Bulletin 76, 1145–1164.

Hudleston, P.J., 1989. The association of folds and veins in shear zones. Journal of Structural Geology 11, 949–957.

Jeffery, G.B., 1922. The motion of ellipsoidal particles immersed in a viscous fluid. Proceedings of the Royal Society London, Series A 102, 161–179.

Koyi, H.A., Skelton, A., 2001. Centrifuge modelling of the evolution of low-angle detachment faults from high-angle normal faults. Journal of Structural Geology 23, 1179–1185.

Mancktelow, N.S., 1991. The analysis of progressive deformation from an inscribed grid. Journal of Structural Geology 13, 853–864.

Mancktelow, N.S., Arbaret, L., Pennacchioni, G., 2002. Experimental observations on the effect of interface slip on rotation and stabilization of rigid particles in simple shear and a comparison with natural mylonites. Journal of Structural Geology 24, 567–585.

Marques, F.O., Coelho, S., 2001. Rotation of rigid elliptical cylinders in viscous simple shear flow: analogue experiments. Journal of Structural Geology 23, 609–617.

Odonne, F., 1990. The control of deformation intensity around a fault: natural and experimental examples. Journal of Structural Geology 12, 911–921.

Passchier, C.W., 2001. Flanking structures. Journal Structural Geology 23, 951–962.

Passchier, C.W., Trouw, R.A.J., 1996. Microtectonics, Springer, Berlin.

Poirier, J.P., 1980. Shear localization and shear instability in materials in the ductile field. Journal of Structural Geology 2, 135–142.

Reches, Z., Eidelman, A., 1995. Drag along faults. Tectonophysics 247, 145–156.

Reiner, M., 1969. Deformation, Strain and Flow, 3rd ed, H.K. Lewis & Co, London, 347pp.

Simpson, C., Schmid, S.M., 1983. An evaluation of criteria to deduce the sense of movement in sheared rocks. Geological Society of America Bulletin 94, 1281–1288.

ten Grotenhuis, S.M., Piazolo, S., Pakula, T., Passchier, C.W., Bons, P.D., 2002. Are polymers suitable rock analogs? Tectonophysics 350, 35–47.

Weijermars, R., 1986. Flow behaviour and physical chemistry of bouncing putties and related polymers in view of tectonic laboratory applications. Tectonophysics 124, 345–358.